Performance evaluation of steel-polypropylene hybrid fiber reinforced concrete under supercritical carbonation

Hao Bao[a], Min Yu[b,*], Yin Chi[b], Yu Liu[b], Jianqiao Ye[c,*]
a. College of Civil Engineering & Architecture, China Three Gorges University, Yichang, China
b. School of Civil Engineering, Wuhan University, Wuhan, China
c. Department of Engineering, Lancaster University, Lancaster LA1 4YR, UK
* Correspondence author: ceyumin@whu.edu.cn (M. Yu), j.ye2@lancaster.ac.uk (J. Ye)

Abstract: In this paper, systematic supercritical carbonation tests of steel-polypropylene hybrid fiber reinforced concrete (SPFRC) were carried out to evaluate the performance of SPFRC under supercritical condition. The effects of the length-diameter ratio of steel fiber, volume fraction of steel fiber, and polypropylene fiber on the carbonation depth and compressive strength of concrete under supercritical condition were studied. A one-dimensional mathematical model for the physical-chemical coupling process of supercritical carbonation of cement-based materials was established. The relational model between the equivalent porosity and the compressive strength of fully carbonated SPFRC was also proposed. Results indicate that whether the addition of steel fibers or polypropylene fibers or the inclusion of fibers can accelerate the carbonation process by the increase of porosity. The carbonation depths of SPFRC increase with the increase of the addition of steel fibers and polypropylene fibers. The compressive strength after carbonation is significantly increased. The maximum relative compressive strength was obtained when the volume fraction of steel fibers and polypropylene fibers were 1.5% and 0.0% and the length-diameter ratio of steel fiber was 60, respectively. Furthermore, a mathematical model was proposed to evaluate the equivalent initial porosity of SPFRC.

Keywords: Steel fibers; Polypropylene fibers; Supercritical carbonation; Carbonation depth; Compressive strength.

1. Introduction

Fiber-reinforced concrete (FRC), a typical engineering material [1], has been extensively utilized in tunnel linings [2], military engineering [3], etc. There are significant advantages in the utilization of FRC. The cracking is prevented by toughening of steel and polypropylene fiber reinforced concrete [4-6], the microstructures of concrete are changed [7, 8], tensile and flexural strength are improved [9, 10]. The material limitations of traditional concrete such as low tensile strength, brittleness, and poor ductility can be avoided by the addition of steel fibers in concrete [11]. The dry shrinkage deformation of concrete can be reduced by the addition of polypropylene fibers in concrete [12]. For reinforced concrete structures, the transport of CO_2 in concrete and the carbonation reaction will convert $Ca(OH)_2$ into $CaCO_3$, reduce the pH value of pore solution, and destroy the passivation film on the surface of steel bars in concrete structures, cause the corrosion of reinforcements [13, 14]. The maximum carbonation rate will be obtained when the relative humidity used for carbonation in a controlled environment ranges from 55% to 70% [15]. However, FRC is a cementitious composite, when FRC structures are subjected to carbonation penetration, the carbon dioxide will react with the alkaline substances in the FRC. The carbonation products, which had a higher molar volume than the original phases [16], could decrease the pore volume and permeability of the concrete products [17]. The capillary porosity, moisture contents and microcracking of FRC are reduced after the CO_2 treatment. CO_2 curing yields better flexural strength [18]. Then the compressive strength was increased and the porosity was reduced [9].

The accelerated carbonation technology had been extensively applied to study the carbonation performance of fiber-reinforced concrete [19]. However, the research period of the accelerated carbonation test ranges from 3 to 24 months, and the corresponding carbonation depth varies between 1 to 10 mm [20]. Meanwhile, with the development of techniques of carbon dioxide storage [21], supercritical carbonation techniques have been applied in the treatment of cement-based materials [22-31] and the seal of heavy metal [16, 32-34]. CO_2 will be in a supercritical fluid condition with the temperature and pressure exceed 304.12 K and 7.38 MPa, respectively [35]. The accomplishment of the carbonation test of concrete can be sharply shortened to almost 7.5 hours with a carbonation depth of 10 mm [36]. Supercritical carbonation techniques have become a promising and time-saving method in the study of carbonation resistance of fiber reinforced concrete. Furthermore, the mechanical properties, microstructural stability [37], and toughness of fiber reinforced concrete can be improved after the supercritical carbonation CO_2 treatment [38]. The supercritical carbonation treatment significantly increased the designed strength and toughness of the fiber-reinforced cement and greatly increased the fiber-matrix bond [39]. However, the addition of steel fibers and polypropylene fibers can increase the CO_2 penetration path and decrease the compactness of the matrix, and then reduce the carbonation resistance of SPFRC. The strengthening mechanism of the supercritical carbonation treatment of SPFRC is indeterminate. The optimal contents of steel and polypropylene fibers are controversial.

Carbonation depth, compressive strength and $Ca(OH)_2$ into $CaCO_3$ conversion are the three main indicators to be concerned for the performance evaluation of the carbonated SPFRC [40, 41]. Whatever natural carbonation, accelerated carbonation, and supercritical carbonation, the average carbonation depth was concerned as one of the factors to evaluate the carbonation degree of concrete [42, 43]. For the corrosion of reinforced concrete, the maximum carbonation depth is more important than the average carbonation depth. Experimental research has shown that under both natural [44] and supercritical [36, 41, 45] conditions, the boundary topography of a carbonation zone is irregular, characterized by a random distribution of depth along the boundary with distinctive maximum and minimum. Meanwhile, the compressive strength of concrete increases after the treatment of carbonation. Due to carbonation, the compressive strength of concrete cured in the accelerated carbonation chamber was higher than that of concrete cured in the general air environment [46]. The compressive strength of concrete increases rapidly at the initial stage of carbonation and increases gradually with the increase of carbonation depth. When the carbonation depth exceeds a certain value, the compressive strength of concrete increases slowly [47]. There is no systematic and in-depth study on the variation of compressive strength and carbonation depth of SPFRC after the supercritical carbonation treatment.

Due to the complex nature of the problem, this paper attempts, as a pioneer work [36, 45, 48], to focus on investigating the performance of steel-polypropylene hybrid fiber reinforced concrete under supercritical carbonation. The supercritical carbonation test of SPFRC with different mix proportions was carried out. The effects of length-diameter ratio of steel fiber, the volume fraction of steel fiber, and polypropylene fiber on the carbonation resistance were discussed. The compressive strength of SPFRC specimens after and without supercritical carbonation was tested. The variation of compressive strength without and after the carbonation of SPFRC specimens with different mix proportions was analyzed. The supercritical carbonation model of

SPFRC was established based on the previous work [41]. The variation of average carbonation depth over time in the process of supercritical carbonation of concrete was simulated and the value of equivalent initial porosity of the matrix of SPFRC was estimated. The influence of types and contents of fibers on the carbonation depth was obtained. The carbonation depth of SPFRC at different initial porosity was studied and the equivalent porosity of SPFRC with different mix proportions was obtained. Besides, the mathematical model of the relationship between the compressive strength and the equivalent porosity of SPFRC after full carbonation was proposed.

2. Experimental program

2.1. Materials and mix design

In the test, Portland cement type P.O 42.5 was used as the binder for the mixes. The chemical components of cement were determined by an X-ray fluorescence spectrometer (XRF) are listed in Table 1. Natural river sands with a fineness modulus of 2.69 and gravels with a size range of 5 mm to 20 mm were used as the fine and coarse aggregates, respectively. The polycarboxylic acid high-performance water reducing agent with a water-reducing rate of 25%~35% was used. The concrete was designed according to the specification for the mix proportion design of ordinary concrete [49] and technical specification for reinforced concrete structures [50] with the designed cube compressive strength of 40 MPa. The corresponding designed mix proportions of concrete are shown in Table 2.

Table 1 Chemical components of cement, in mass percent (%).

SiO_2	Al_2O_3	Fe_2O_3	CaO	MgO	SO_3	R_2O
21.7	4.84	3.19	62.26	2.35	3.57	2.09

Remarks: R_2O defines the general term for oxides with very little content.

Table 2 Mix proportions of concrete.

Components Unit	Cement (kg/m^3)	Gravel (kg/m^3)	Sand (kg/m^3)	Water (kg/m^3)	Water-binder ratio -
Concrete	417	1086	724	175	0.42

The shear wave steel fibers with the length-diameter ratio of 30, 60, 80, polypropylene fibers with a length of 11 mm, and the coarse aggregates were prepared for the experiment. The physical and mechanical properties of steel fibers and polypropylene fibers were shown in Table 3.

Table 3 Physical and mechanical properties of steel fibers and polypropylene fibers.

Type of fibers	Equivalent diameter	Density (g/cm^3)	Compressive strength (MPa)
Shear wave fiber	0.55 mm	7.8	≥600
Bunchy monofilament fiber	18μm ~48μm	0.91	≥450

2.2. Specimens preparation

To study the effects of the supercritical carbonation on the carbonation mechanism of steel-polypropylene hybrid fiber reinforced concrete, the parameters considered in this study include fiber type, the volume fraction of fiber, length-diameter ratio of steel fiber. The compressive strength of concrete and the specimen's design of steel-polypropylene hybrid fiber reinforced concrete (SPFRC) were summarized and shown in Table 4.

Table 4 Specimens design of SPFRC.

Group number	Length-diameter ratio of steel fiber, λ_{SF}	Volume fraction of steel fiber, ρ_{SF}	Volume fraction of polypropylene fiber, ρ_{PF}
SPFRC0000(60)	60	0	0
SPFRC0500(60)	60	0.5%	0
SPFRC1000(60)	60	1.0%	0
SPFRC1500(30)	30	1.5%	0
SPFRC1500(60)	60	1.5%	0
SPFRC1500(80)	80	1.5%	0
SPFRC0005(60)	60	0	0.05%
SPFRC0505(60)	60	0.5%	0.05%
SPFRC1005(60)	60	1.0%	0.05%
SPFRC1505(60)	60	1.5%	0.05%
SPFRC0010(60)	60	0	0.1%
SPFRC0510(60)	60	0.5%	0.1%
SPFRC1010(60)	60	1.0%	0.1%
SPFRC1510(30)	30	1.5%	0.1%
SPFRC1510(60)	60	1.5%	0.1%
SPFRC1510(80)	80	1.5%	0.1%
SPFRC0015(60)	60	0	0.15%
SPFRC0515(60)	60	0.5%	0.15%
SPFRC1015(60)	60	1.0%	0.15%
SPFRC1515(60)	60	1.5%	0.15%

Remarks: As shown in SPFRC1505(60), SPFRC represents the steel-polypropylene hybrid fiber reinforced concrete. 15 represents the volume fraction of steel fiber is 15%. 05 represents the volume fraction of polypropylene fiber is 5%. 60 represents the length-diameter ratio of steel fiber is 60.

A standard slump flow test was conducted to measure the slump of all mixtures [51]. The top diameter, bottom diameter, and height of the slump cone were 100 mm, 200 mm, and 300 mm, respectively. The slump cone was placed on the plate and the fresh SPFRC was cast into the slump cone fully. Then, the slump cone was left vertically and smoothly to allow the concrete mixture to flow out freely. The lifting process of the slump cone was completed in 5 seconds. The final diameter of the concrete mixture after slump flow was measured by the steel ruler, and the measurement was carried out in two directions perpendicular to each other, and the average value of the two measured diameters was taken as the value of slump flow. The target slump is 30 mm.

Steel-polypropylene hybrid fiber reinforced concrete cubes with a dimension of 100 mm × 100 mm × 100 mm were designed for the experiments of supercritical carbonation. 20 groups of SPFRC specimens with four different volume fractions of steel fiber (ρ_{SF} = 0, 0.5%, 1.0%, 1.5%), four different volume fractions of polypropylene fiber (ρ_{PF} = 0, 0.05%, 0.10%, 0.15%) and three different length-diameter ratios of steel fiber (λ_{SF} = 30, 60, 80) were cast. There are nine SPFRC specimens in each group and the total number of specimens is 180. Three of them were carbonated for the measurement of carbonation depth. Another three were carbonated for the measurement of compressive strength after the carbonation of concrete. The remaining three specimens were not carbonated for the measurement of the compressive strength of concrete without carbonation. After casting, the test specimens were covered with plastic sheets and left in the casting room for 24 hrs. The specimens were then demolded and placed into a standard curing room with a constant temperature of 20 ℃ and humidity of 95% until 28-day strength was achieved. The specimens were taken out and placed in the temperature and humidity control chamber for further curing for 28 days after the 28 days of curing in the standard curing room. The relative humidity was set at 70% to control the initial water retention rate of the concrete specimens. The average value of the recorded relative humidity was 68.4%.

2.3. Experimental program

2.3.1. Supercritical carbonation of SPFRC

To monitor the supercritical carbonation test process of steel-polypropylene hybrid fiber reinforced concrete more efficiently, the supercritical carbonation device was applied in the test. CO_2 can be compressed into the supercritical condition and the steel-polypropylene hybrid fiber reinforced concrete can be carbonated. The details of the closed-cycle carbonation device are shown in Fig. 1 (a). During supercritical carbonation of SPFRC specimens, the temperature and pressure in the reaction still were controlled by temperature and pressure controller as shown in Fig. 1 (b) and (c), respectively, and detected by the temperature sensor and the pressure gauge, respectively. The recirculated water and heating rods can be utilized to control the temperature in the reaction still. More details of this supercritical carbonation system are shown in previous work [36].

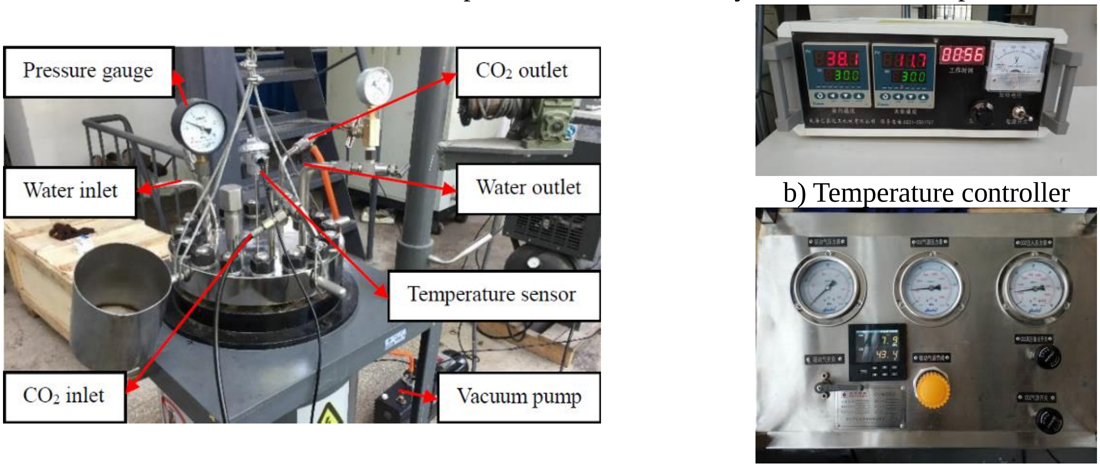

a) Reaction still b) Temperature controller c) Pressure controller

Fig. 1. Closed-cycle carbonation setup.

The main experiment procedure of supercritical carbonation of steel-polypropylene hybrid fiber reinforced concrete is shown as follows [36]:

1) Six concrete cubes were placed on the bracket as shown in Fig. 2 (a).

2) The bracket with the specimens was placed in the reaction still as shown in Fig. 2 (b).

3) The reaction still was vacuumed to almost -1.00 bar after the seal of the chamber as shown in Fig. 2 (c).

4) The injection of CO_2 in the CO_2 tanks to the reaction still by an air compressor until the accomplishment and maintaining of the target pressure and temperature in the reaction still.

5) The CO_2 gas was driven from the reaction still to the CO_2 tanks by the air compressor to realize the recycling of CO_2.

6) The six carbonated steel-polypropylene hybrid fiber reinforced concrete cubes were removed from the reaction still.

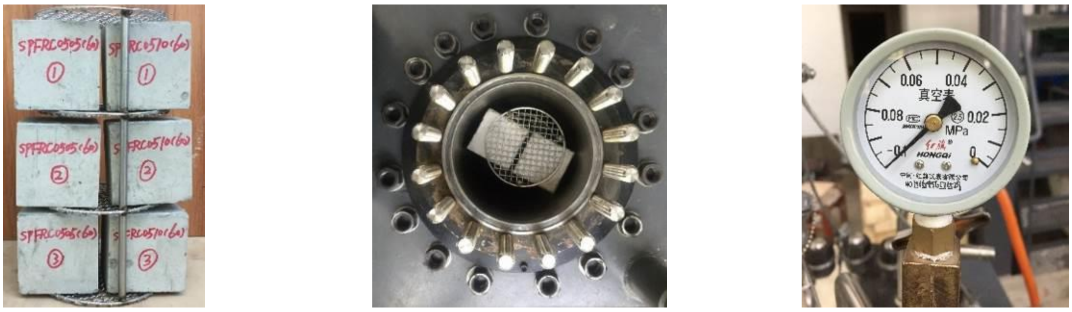

a) Specimens on the bracket b) Specimens in the reaction still c) Negative pressure gauge

Fig. 2. Preparation of the supercritical carbonation of SPFRC.

In the supercritical carbonation test, the designed pressure and temperature are 8.0 MPa and 40℃, respectively. From the pre-carbonation results, it is observed that a minimum of 5-6 hours of supercritical carbonation time was required for reliable data processing, longer carbonation time would lead to complete carbonation with no or very short carbonation boundary to be analyzed. Therefore, the designed supercritical carbonation time was six hours. During the procedure of supercritical carbonation of steel-polypropylene hybrid fiber reinforced concrete, the temperature and pressure were monitored. Without loss of generality, only partial recorded temperature and pressure of SPFRC specimens during the supercritical carbonation process were shown in Fig. 3. As can be seen from Fig. 3, the pressure and temperature in the reaction still can be controlled stably by the closed-cycle carbonation setup.

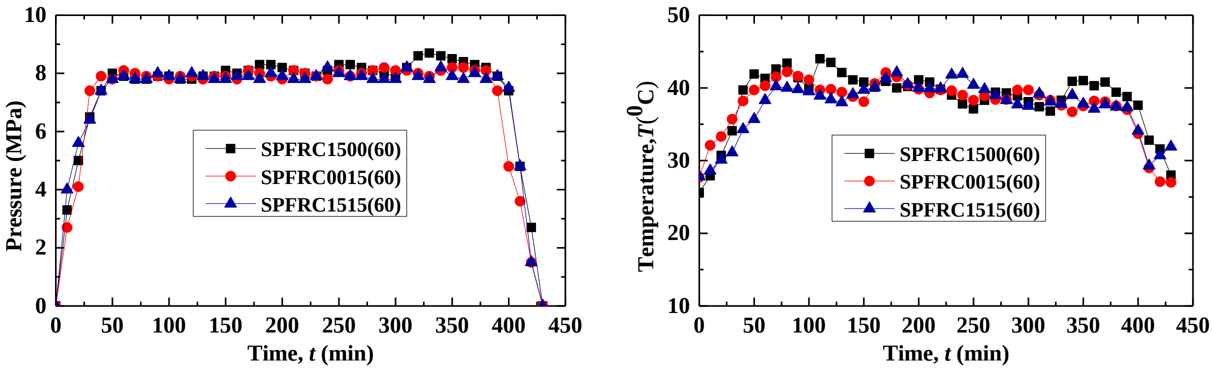

(a) Pressure (b) Temperature

Fig. 3. Carbonation condition of SPFRC: Carbonated for 7.17 h (supercritically carbonated for 6 h).

2.3.2. SEM observation

To study the effect of steel fibers and polypropylene fibers on the carbonation boundaries microcosmically, the SPFRC samples without and after the achievement of supercritical carbonation were tested by Scanning Electron Microscopy (SEM). The microtopography of steel fiber, polypropylene fiber, matrix, and cracks was also observed. Before the observation, some carbonated SPFRC samples were received cutting and sanding with the power tool and then the fresh cuts of the cubes were polished and cleaned to avoid the effect of dust on observation results. The effect of the distribution of steel fibers and polypropylene fibers near the boundary between the carbonation zone and non-carbonation zone of concrete on the carbonation depth is the focus of the observation. Finally, the samples were prepared to observe the microstructure of matrix, steel fibers, and polypropylene fibers by the SEM test. The prepared samples were dried in an oven to a constant weight and the surfaces of the samples were coated with gold powder in an ion spatter to increase their conductivity. The samples were vacuumed after the placement of samples on the stage of a scanning electron microscope. Then the contrast, brightness, the best multiple and rate of scanning were adjusted and determined. The images were taken on a JSM-7500F equipped with a tungsten filament. In the process of samples preparation and testing, the integrity and health of the samples were guaranteed.

2.3.3. Compressive strength testing

After the accomplishment of the supercritical carbonation test of SPFRC, partial specimens were prepared to obtain the compressive strength of SPFRC after the carbonation. The compressive strength test of SPFRC cubes was measured using a 3000 kN MTS YAW6306 testing machine according to the test methods used for steel fiber reinforced concrete (CECS 13: 2009) [51]. The loading rate is 1.2 MPa/s. The ends of the specimens were polished smoothly to avoid the influence of stress concentration on the compressive behavior of the specimens before the compressive strength testing. The compressive loads and corresponding displacements were automated recorded by the testing system. The ultimate compressive loads were also obtained.

3. Results and discussion

3.1. Carbonation results

The carbonation depth of concrete specimens was measured and compared in this Section. After the achievement of the supercritical carbonation of SPFRC specimens, the carbonated concrete cubes were removed from the reaction still. Then some of the specimens were cut into two halves with a precise power cutting tool. The appropriate cutting speed was determined as 1 mm/s according to the preliminary experiment. The steel fibers and polypropylene fibers in concrete can be completely cut off. The pullout and fracture of fibers and the debonding of the interface between cement matrix and fibers can be avoided. The fresh cuts of the samples were polished and cleaned. Then the phenolphthalein solution was sprinkled homogeneously on the cutting surface. The carbonation boundary can be identified after the accomplishment of the color reaction. The carbonation profiles can be obtained by a scanner [36]. The enlarged details of the carbonation profile of partial SPFRC specimens were shown in Fig. 4. As shown in Fig. 4, the random nature of carbonation boundaries not only can be affected by the random distribution of porosity and coarse aggregates [36, 42] but also affected by the existence of steel fibers. However, the effect of polypropylene fibers on the distribution of carbonation depth cannot be macroscopically observed.

(a) SPFRC0000(60) (b) SPFRC0500(60) (c) SPFRC1510(80)

Fig. 4. Zoomed-in details of test carbonation profile of partial SPFRC specimens.

The depiction in the outline of the scanned profiles and carbonation boundaries are shown in Figs. (5-7), respectively. Fig. 5 shows the carbonation depth of steel-polypropylene hybrid fiber reinforced concrete cubes with various volume fractions of steel fibers and a fixed length-diameter ratio of steel fibers of 60. Fig. 6 shows the carbonation depth of steel-polypropylene hybrid fiber reinforced concrete cubes with a various volume fractions of polypropylene fibers and a fixed length-diameter ratio of steel fibers of 60. Fig. 7 shows the carbonation depth of steel-polypropylene hybrid fiber reinforced concrete cubes with various length-diameter ratios of steel fibers. As shown in Figs. (5-7), there are irregular carbonation boundaries around the non-carbonated zone.

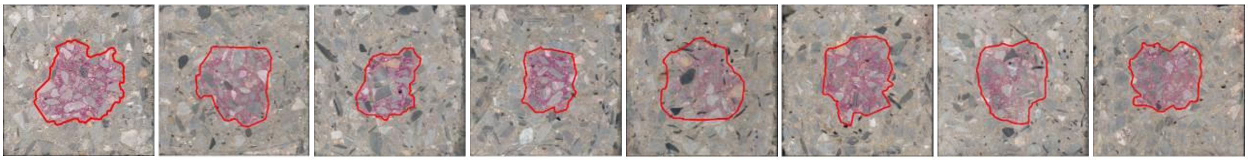

ρ_{SF} = 0 ρ_{SF} = 0.5% ρ_{SF} = 1.0% ρ_{SF} = 1.5% ρ_{SF} = 0 ρ_{SF} = 0.5% ρ_{SF} = 1.0% ρ_{SF} = 1.5%

a) ρ_{PF} = 0, λ_{SF} = 60 b) ρ_{PF} = 0.05%, λ_{SF} = 60

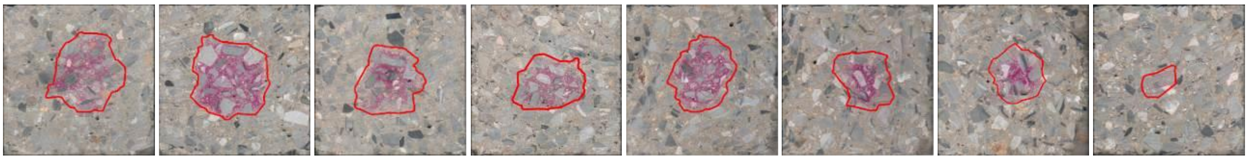

ρ_{SF} = 0 ρ_{SF} = 0.5% ρ_{SF} = 1.0% ρ_{SF} = 1.5% ρ_{SF} = 0 ρ_{SF} = 0.5% ρ_{SF} = 1.0% ρ_{SF} = 1.5%

c) ρ_{PF} = 0.10%, λ_{SF} = 60 d) ρ_{PF} = 0.15%, λ_{SF} = 60

Fig. 5. The carbonation depth of steel-polypropylene hybrid fiber reinforced concrete cubes with various volume fractions of steel fibers.

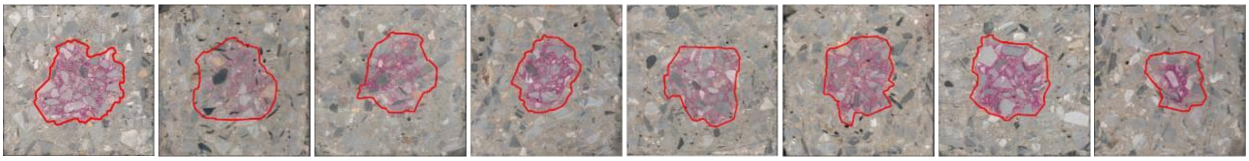

ρ_{PF} = 0 ρ_{PF} = 0.05% ρ_{PF} = 0.10% ρ_{PF} = 0.15% ρ_{PF} = 0 ρ_{PF} = 0.05% ρ_{PF} = 0.10% ρ_{PF} = 0.15%

a) ρ_{SF} = 0, λ_{SF} = 60 b) ρ_{SF} = 0.5%, λ_{SF} = 60

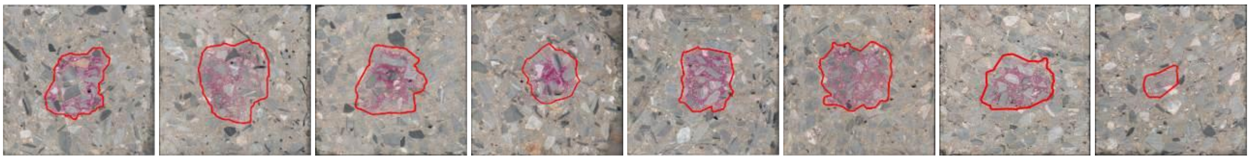

ρ_{PF} = 0 ρ_{PF} = 0.05% ρ_{PF} = 0.10% ρ_{PF} = 0.15% ρ_{PF} = 0 ρ_{PF} = 0.05% ρ_{PF} = 0.10% ρ_{PF} = 0.15%

c) ρ_{SF} = 1.0%, λ_{SF} = 60 d) ρ_{SF} = 1.5%, λ_{SF} = 60

Fig. 6. The carbonation depth of steel-polypropylene hybrid fiber reinforced concrete cubes with various volume fractions of polypropylene fibers.

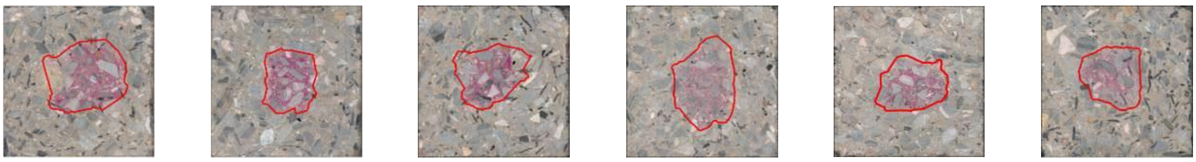

λ_{SF} = 30 λ_{SF} = 60 λ_{SF} = 80 λ_{SF} = 30 λ_{SF} = 60 λ_{SF} = 80

(a) ρ_{SF} = 1.5%, ρ_{PF} = 0 (b) ρ_{SF} = 1.5%, ρ_{PF} = 0.10%

Fig. 7. The carbonation depth of steel-polypropylene hybrid fiber reinforced concrete cubes with various length-diameter ratios of steel fibers.

It can be generally concluded that the carbonated areas increase with the increase of the volume fraction of steel fibers or polypropylene fibers according to the carbonation results in Fig. 5 and Fig. 6. The effect of the addition of fibers on the random nature of the carbonated areas cannot be ignored. The increase of volume fraction of fibers increases the length and area of the weak interface transition zone between the fibers and cement matrix, leading to faster transport of CO_2 and more rapid carbonation in SPFRC [8, 52]. As shown in Fig. 7, the maximum carbonated areas were obtained when the length-diameter ratio of steel fibers is 60.

To statistically and quantitatively analyze the effect of steel fibers and polypropylene fibers on the carbonated areas, the distribution of the measured carbonation depths along the carbonation zone was obtained by the imaging processing technique [36]. The illustration of the process of carbonation results of SPFRC was concluded and shown in Fig. 8. More details about the image processing of the irregular carbonation profiles can be found in the previous work [36]. Finally, the results of the carbonation depth of SPFRC after supercritical carbonation were shown in Table 5.

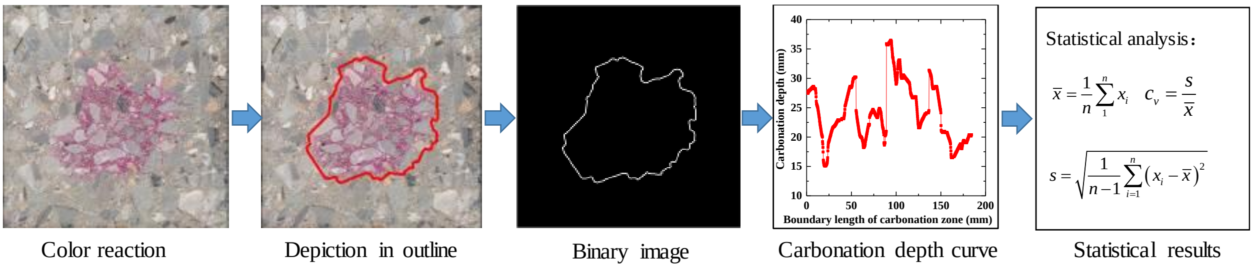

Fig. 8. Illustration of the process of carbonation results of SPFRC.

Table 5 Results of supercritical carbonation depth of SPFRC.

Specimens number	Average carbonation depth (mm)	Coefficient of variation	Specimens number	Average carbonation depth (mm)	Coefficient of variation
SPFRC0000(60)	23.47	0.20	SPFRC0010(60)	24.98	0.23
SPFRC0500(60)	23.71	0.11	SPFRC0510(60)	27.90	0.11
SPFRC1000(60)	24.41	0.11	SPFRC1010(60)	28.99	0.12
SPFRC1500(30)	28.04	0.19	SPFRC1510(30)	25.93	0.18
SPFRC1500(60)	25.86	0.16	SPFRC1510(60)	30.53	0.13
SPFRC1500(80)	30.04	0.20	SPFRC1510(80)	30.94	0.12
SPFRC0005(60)	23.80	0.12	SPFRC0015(60)	28.68	0.14
SPFRC0505(60)	26.66	0.18	SPFRC0515(60)	32.51	0.14
SPFRC1005(60)	25.66	0.17	SPFRC1015(60)	34.26	0.11
SPFRC1505(60)	28.27	0.15	SPFRC1515(60)	39.56	0.14

3.2. Effect of supercritical carbonation on the microstructure of SPFRC

The SEM images of a typical area of the steel fiber, polypropylene hybrid fiber, cracks, and the matrix with the magnification times of 100 are shown in Fig. 9. The microstructure of steel fiber reinforced concrete with the number of the specimen of SPFRC1500(60) without and after the carbonation treatment are shown in Figs. 9 (a) and (b), respectively. The microcracks (Fig. 9a) occurred along the narrow gap between the matrix and steel fiber without carbonation can be seen, while no cracks along the boundary between matrix and steel fiber can be observed (Fig. 9b) and the matrix attached to the steel fiber firmly after carbonation. This indicates that the porosity or cracks between the matrix and steel fiber can be reduced by the supercritical carbonation treatment. The microtopography of polypropylene hybrid fiber reinforced concrete (SPFRC0015(60)) without and after carbonation is shown in Figs. 9 (c) and (d), respectively. The cracks around the polypropylene hybrid fiber can be observed without and after carbonation. However, the width of the cracks was reduced after supercritical carbonation treatment. Without loss of generality, the SEM images of SPFRC1515(60) without and after carbonation treatment were shown in Figs. 9 (e) and (f), respectively. Also, the supercritical carbonation treatment can reduce the cracks between the matrix and steel fibers or polypropylene hybrid fibers to some extent. The weakness of the interfacial transition zone between the cement matrix and fibers may shorten the transport time of CO_2, leading to more rapid carbonation in the ITZ [8, 52]. The existence of steel fibers and polypropylene fibers in the SPFRC may result in the random nature of carbonation boundaries.

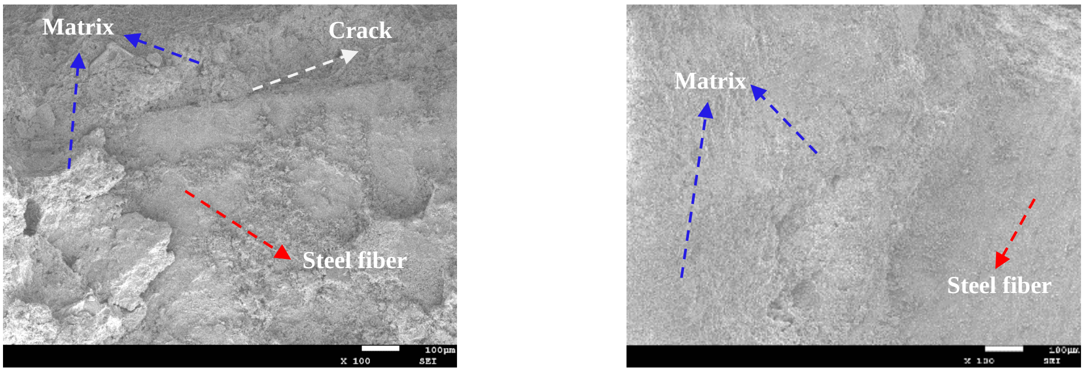

a) Steel fiber reinforced concrete without carbonation (SPFRC1500 (60))   b) Steel fiber reinforced concrete after carbonation (SPFRC1500 (60))

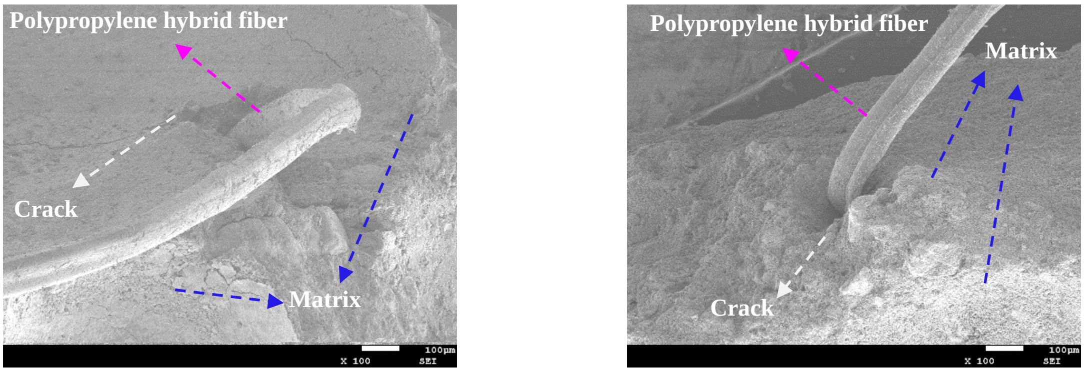

c) Polypropylene hybrid fiber reinforced concrete without carbonation (SPFRC0015(60))   d) Polypropylene hybrid fiber reinforced concrete after carbonation (SPFRC0015(60))

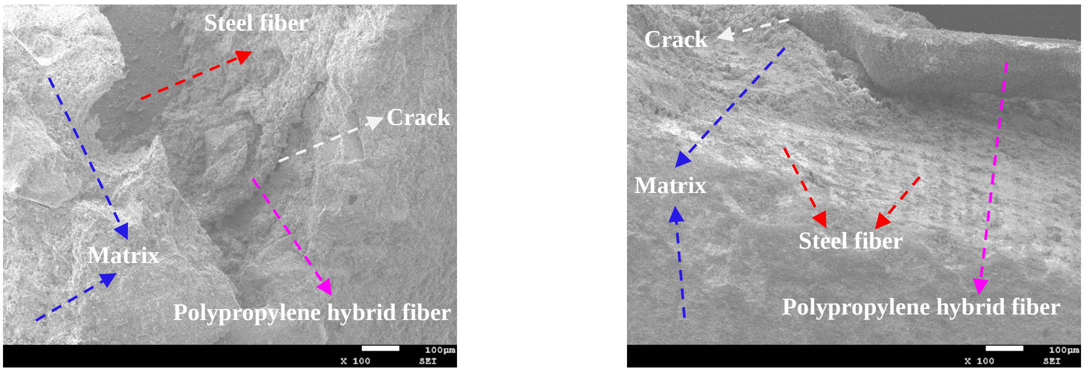

e) Steel-polypropylene hybrid fiber reinforced concrete without carbonation (SPFRC1515(60))   f) Steel-polypropylene hybrid fiber reinforced concrete after carbonation (SPFRC1515(60))

Fig. 9. SEM micrographs of steel-polypropylene hybrid fiber reinforced concrete samples without and after supercritical carbonation.

3.3. Effects of fibers on the carbonation depth of SPFRC under supercritical condition

3.3.1. Effect of steel fibers

The comparison of the carbonation depth of SPFRC with different volume fractions of steel fibers under supercritical condition is shown in Fig. 10. It can be concluded that the carbonation of concrete is generally accelerated by the addition of steel fibers in the SPFRC for the average carbonation depth of concrete increases with the increase of volume fraction of steel fibers. In Fig. 10, the colored lines and symbols show the average carbonation depth and the error bars represent the minimum and maximum carbonation depth. The maximum and minimum carbonation depths are discrete with the increase of volume fraction of steel fibers, which may be caused by the random nature of the distribution of carbonation depth and limited experimental data. The maximum and minimum carbonation depth are fluctuant with the increase of volume fraction of steel fiber for the experimental error, positive or negative hybrid effect [53] or the deterioration of liquidity, increase of imperfection and porosity of concrete by the caking and sinkage of steel fibers and floating of coarse aggregates [54]. The fluctuation of minimum and maximum carbonation depth may also be caused by the variation of consistency and workability of SPFRC with different volume fractions of steel fibers and polypropylene fibers and the change of porosity during the curing and supercritical carbonation of SPFRC.

,

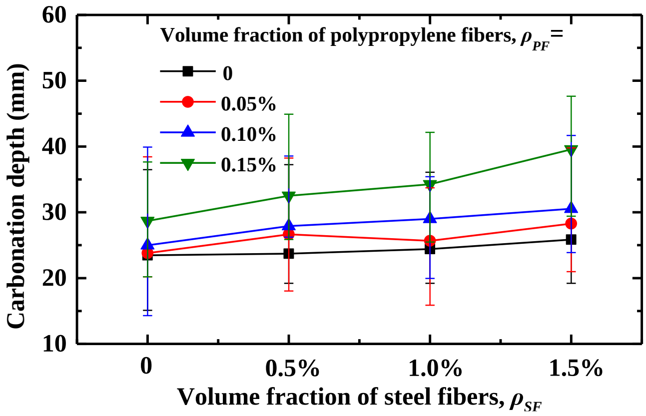

Fig. 10. Influence curves of volume fraction of steel fibers on carbonation depth (λ_{SF} =60).

SPFRC1500 and SPFRC1510 were taken as examples to analyze the effect of the length-diameter ratio of steel fiber on the supercritical carbonation depth of concrete. The influence curve of length-diameter ratio of steel fibers on carbonation depth was shown in Fig. 11. The carbonation resistance is enhanced with the increase of the length-diameter ratio of steel fibers within a certain range from 30 to 60, but a further increase of the length-diameter ratio of steel fibers from 60 to 80 will reduce the carbonation resistance. The carbonation resistance of a length-diameter ratio of 60 is better than that of 30 or 80. The error bars show that the effect of the length-diameter ratio of steel fibers on the maximum and minimum carbonation depth is not obvious for the random distribution of coarse aggregates and fibers. As shown in Fig. 11, the maximum carbonated areas were obtained when the length-diameter ratio of steel fibers is 60. It is possible that when the length-diameter ratio of steel fibers is 30, the effect of fibers on the carbonated areas is not as great as that of coarse aggregates. In addition, when the length-diameter ratio of steel fibers is 80, the ITZ between fibers and matrix is filled with calcium carbonates produced by the reaction of calcium hydroxide and CO_2. Then the reaction rate of carbonation and the carbonated areas are reduced. The hybrid of steel fibers and polypropylene fibers increases the defects of the matrix and leads to the significant carbonation of concrete.

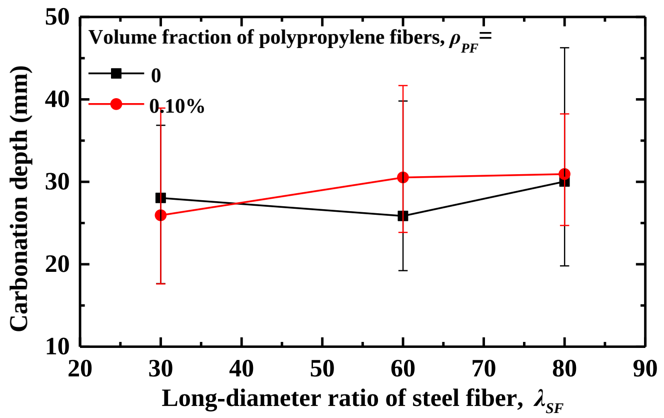

Fig. 11. Effect curves of the length-diameter ratio of steel fibers on carbonation depth (ρ_{SF} = 1.5%).

3.3.2. Effect of polypropylene fibers

The comparison of the carbonation depth of SPFRC with different volume fractions of polypropylene fibers under supercritical condition is shown in Fig. 12. The colored lines and symbols also show the average carbonation depth and the error bars represent the minimum and maximum carbonation depth. In general, the average carbonation depth increase with the increase of the addition of polypropylene fibers. When the volume fraction of polypropylene fibers is below 0.05%, the effect of polypropylene fibers on the average carbonation depth is not obvious. Also, there is no significant effect of the volume fraction of polypropylene fibers on the maximum and minimum carbonation depth of SPFRC.

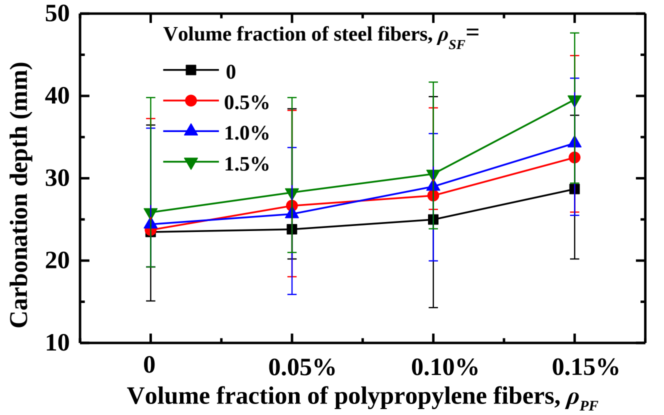

Fig. 12. Influence curves of volume fraction of polypropylene fibers on carbonation depth (λ_{SF} =60).

3.4. Compressive strength of SPFRC after supercritical carbonation

3.4.1. Results of compressive strength before and after supercritical carbonation

Without loss of generality, the failure pattern of typical SPFRC specimens was shown in Fig. 13. It can be concluded that the addition of steel fibers or polypropylene fibers can prevent the disintegration of specimens to some extent by comparing the failure pattern of specimens in Figs. 13 (a-c). In the meantime, the integrity of the specimen can be better ensured by the addition of polypropylene fibers than steel fibers. This may be attributed to the more uniform distribution of polypropylene fibers, which decreases the propagation of the fracture plane [55]. As shown in Fig. 13, the failure pattern of SPFRC specimens demonstrated that the fracture plane propagates through the cement paste. The compressive strength of SPFRC depends strongly on the cement paste. The toughness of concrete was improved by the addition of steel fibers or polypropylene fibers for the bridging effect of fibers across cracks [56]. The crack propagation was retarded, and the fracture plane was bridged by fibers [57].

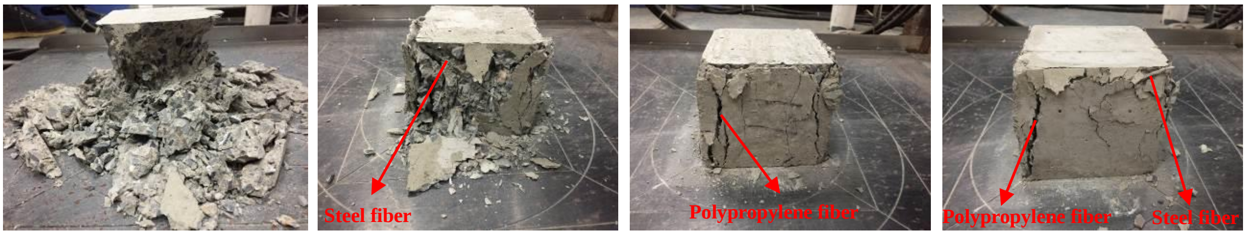

a) SPFRC0000(60) b) SPFRC1500 (60) c) SPFRC0015(60) d) SPFRC1015(60)

Fig. 13. Failure pattern of SPFRC.

The relative compressive strength was proposed to evaluate the effect of carbonation on the compressive properties of a cement-based material. It is a specific value of the compressive strength of concrete cubes after carbonation and without carbonation. It is defined as the following equation [58]:

$$k_{RC} = \frac{f_{CC}}{f_{CO}} \tag{1}$$

where k_{RC} is the parameter of relative comprehensive compressive strength. f_{CO} and f_{CC} are the comprehensive compressive strength of specimens without and after carbonation with the unit of MPa, respectively. The partially carbonated cubes can be regarded as the combination of a fully carbonated shell and a non-carbonated core. Therefore, f_{CC} is the comprehensive compressive strength of carbonated parts and non-carbonated parts after the carbonation of concrete.

The effect of carbonation on the compressive properties of cement-based material cannot be accurately calculated by Eq. (1). To calculate the compressive strength of concrete cubes after carbonation more accurately, the compressive strength of concrete was defined comprehensively in Eq. (2).

$$f_{CC} = \frac{f_{CO}A_{CO} + f_{CC}'A_{CC}}{A_{CO} + A_{CC}} \tag{2}$$

where f_{CC}' is the compressive strength of fully carbonated concrete cubes with the unit of MPa. A_{CO} is the area of the non-carbonated zone with the unit of m^2 and the value was obtained by the calculation of the area circled by the red curve as shown in Figs. (5-7); A_{CC} is the sectional area of the fully carbonated shell with the unit of m^2 and the value was obtained by the difference of the sectional area of the cube and A_{CO}.

It is worth emphasizing that the compressive strength of fully carbonated concrete, f_{CC}', can be calculated according to Eq. (2) and the other parameters can be obtained from the test results. The compressive strength of SPFRC without and after carbonated were obtained and shown in Table 6.

Table 6 Compressive strength of SPFRC.

Specimens number	f_{CO} (MPa)	f_{CC} (MPa)	f_{CC}/f_{CO}	$A_{CO}\times10^{-3}$ (m^2)	$A_{CC}\times10^{-3}$ (m^2)	f_{CC}' (MPa)	f_{CC}'/f_{CO}
SPFRC0000(60)	39.6	55.8	1.41	2.478	7.522	61.1	1.54
SPFRC0500(60)	37.6	49.5	1.32	1.221	8.779	51.2	1.36
SPFRC1000(60)	33.4	46.1	1.38	1.428	8.572	48.2	1.44
SPFRC1500(30)	36.2	45.8	1.27	1.820	8.180	47.9	1.32
SPFRC1500(60)	34.3	56.4	1.64	2.045	7.955	62.1	1.81
SPFRC1500(80)	39.6	52.8	1.33	1.515	8.485	55.2	1.39

SPFRC0005(60)	35.0	49.4	1.41	1.756	8.244	52.5	1.50
SPFRC0505(60)	37.5	47.7	1.27	1.999	8.001	50.2	1.34
SPFRC1005(60)	40.9	51.8	1.27	2.367	7.633	55.2	1.35
SPFRC1505(60)	35.3	52.2	1.48	2.015	7.985	56.5	1.60
SPFRC0010(60)	41.1	53.3	1.30	1.993	8.007	56.3	1.37
SPFRC0510(60)	35.6	47.7	1.34	1.555	8.445	49.9	1.40
SPFRC1010(60)	38.8	51.2	1.32	1.829	8.171	54.0	1.39
SPFRC1510(30)	41.9	54.3	1.30	1.862	8.138	57.1	1.36
SPFRC1510(60)	36.1	55.1	1.53	1.324	8.676	58.0	1.61
SPFRC1510(80)	31.2	46.1	1.48	1.298	8.702	48.3	1.55
SPFRC0015(60)	24.9	38.7	1.55	1.505	8.495	41.1	1.65
SPFRC0515(60)	24.3	30.8	1.27	1.187	8.813	31.7	1.30
SPFRC1015(60)	24.7	29.7	1.20	0.872	9.128	30.2	1.22
SPFRC1515(60)	22.9	30.3	1.32	0.369	9.631	30.6	1.34

As shown in Table 6. The compressive strength value of fiber reinforced concrete varies with the variation of volume fraction of steel fibers, volume fraction of polypropylene fiber, and length-diameter ratio of steel fiber. The ultimate compressive strength of SPFRC decreased with the increase of the addition of steel fibers, polypropylene fibers, and the length-diameter ratio of steel fiber before the supercritical carbonation. This may be attributed to the increase of ITZ between the fibers and matrix with the addition of fibers in SPFRC [8]. However, the ultimate compressive strength of SPFRC increased by 22% to 81% after the supercritical carbonation. This may be attributed to the micro-pores of the matrix and ITZ were filled with the calcium carbonate after the carbonation reaction of fiber reinforced concrete, which makes the composite more compacted and increases the fiber-matrix bond [39]. Thus, the ultimate compressive strength of SPFRC increases to some extent. The compressive strength of concrete is affected by supercritical carbonation. The value of the relative compressive strength of concrete is greater than 1. The compressive strength of concrete has been greatly improved after carbonation. The compressive strength and the relative compressive strength of carbonated parts are greater than the overall compressive strength and overall relative compressive strength.

3.4.2. Establishment of mathematical model for the supercritical carbonation of SPFRC

The effect of the initial porosity of hybrid fiber reinforced concrete on the carbonation depth was analyzed in this section. The initial porosity of different hybrid fiber concrete was calibrated through the comparison of test and numerical average carbonation depth. A one-dimensional mathematical model for the physical-chemical coupling process of supercritical carbonation of cement-based materials was established. The change of average carbonation depth over time in the process of supercritical carbonation of concrete was simulated by using multi-physics coupling simulation software. The theoretical model is validated by the test results.

The governing equations for the supercritical carbonation of SPFRC are shown in Eqs. (3-7). The rate of chemical reaction, mass conservation for gas-liquid two phase flow, diffusion and dispersion of CO_2 in water, energy conservation for porous medium, and the solubility of CO_2 in water are all considered in the mathematical model.

$$\frac{\partial R_c}{\partial t} = \alpha_1 \times f_1(h) \times f_2(g_v) \times f_3(R_c) \times f_4(T) \tag{3}$$

$$\frac{\partial(g)}{\partial t}=\frac{\partial(m_{co_2})}{\partial t} \tag{4}$$

$$\frac{\partial(nS_\alpha\rho_\alpha)}{\partial t}+\nabla\cdot(\rho_\alpha\vec{u}_\alpha)=q_\alpha \tag{5}$$

$$\vec{u}_\alpha=-\frac{k_0\left(\frac{n}{n_0}\right)^3\cdot\left(\frac{1-n_0}{1-n}\right)^2k_{r\alpha}}{\mu_\alpha}(\nabla P_\alpha-\rho_\alpha\vec{g}) \tag{6}$$

$$\left(\rho C_q\right)_{eff}\frac{\partial T}{\partial t}=\nabla\cdot\left(k_{eff}\nabla T\right)-\left(C_g\rho_g\vec{u}_g+C_w\rho_w\vec{u}_w\right)\nabla T \tag{7}$$

where R_c is the degree of carbonation; g is the mass concentration of CO_2 in water; n is the porosity of material that decreases during carbonation; P_α is the pressure of phase α; subscript α refers to w for the liquid phase and g for the gaseous phase. The detailed information about the other parameters can be found in Zha [41] and Yu [45].

The initial and boundary conditions were applied to solve the governing equations. In this study, the conditions are introduced and shown in Eqs. (8-10).

$$R_c=R_{c0}=0,\ P_g=P_{g0},\ P_w=P_{w0},\ g=g_0=0,\ T=T_0,\ t=0\ on\ \Omega \tag{8}$$

$$\vec{n}\cdot\nabla R_c=0,\ \vec{n}\cdot\nabla g=0\ on\ \Gamma_2 \tag{9}$$

$$P_g=P_{g,sur},\ P_w=P_{w,sur},\ T=T_{sur}\ on\ \Gamma_1 \tag{10}$$

where R_{c0} is the initial conditions specifying the degree of carbonation; P_{g0} and P_{w0} are the initial water pressure and initial gas pressure, respectively; g_0 is the initial concentration of dissolved CO_2 in water; T_0 is the initial temperature; $\vec{n}$ is the normal vector of the boundary; Γ_2 and Γ_1 are the boundary using Neumann's conditions and Dirichlet's conditions, respectively; $P_{g,sur}$ and $P_{w,sur}$ are the surrounding gas and liquid pressure, respectively; T_{sur} is the surrounding temperature. The detailed information about the other parameters can be found in Zha [41] and Yu [45].

The cement-based materials can be considered as a porous medium. The transformation of carbon dioxide in the pore and the ultimate carbonation results are affected by its related material physical parameters, such as initial porosity, intrinsic permeability rate, and initial saturation. The physical characteristic parameters of cement-based materials in the numerical model are evaluated and shown in Table 7. The control equations, initial conditions, and boundary conditions are given [41, 45]. According to the test procedure, the total carbonation time is 7.17 hours and the supercritical carbonation time is 6 hours. The recorded temperature and pressure of SPFRC specimens during the supercritical carbonation process were applied in the numerical carbonation model.

Table 7 Parameters for SPFRC.

Porous porosity	Value	References
Intrinsic permeability, k_0	10×10^{-21}m^2	[59]
Initial average porosity, n_0	0.13	[59]
Capillary pressure curve coefficient, α	5.3695×10^{-8} Pa^{-1}	[60]
Relative permeability coefficient, m	0.4396	[60]
Relative humidity, h_0	0.684	

As the porosity of concrete range from 0.09 to 0.21 [61], the simulation results of average carbonation depth of SPFRC under supercritical condition with the assumed initial porosity of 0.12, 0.13, 0.14, 0.15, 0.16, 0.17, 0.18, 0.19, 0.20 were calculated as 23.02 mm, 25.26 mm, 27.5 mm, 29.74 mm, 31.98 mm, 34.22 mm, 36.46 mm, 38.7 mm and 40.94 mm, respectively. The test results of the average carbonation depth of the 20 kinds of mixed steel-polypropylene hybrid fiber reinforced concrete under supercritical condition were compared with the numerical results. After the comparison and analysis of experimental and numerical carbonation depth of SPFRC under supercritical carbonation, the value of the initial porosity of hybrid fiber concrete can be estimated by using linear interpolation. The estimated value of the equivalent porosity was obtained and shown in Table 8.

Table 8 Estimated value of equivalent initial porosity.

Specimens number	Estimated value of equivalent initial porosity, n_0	Specimens number	Estimated value of equivalent initial porosity, n_0
SPFRC0000(60)	0.122	SPFRC0010(60)	0.129
SPFRC0500(60)	0.123	SPFRC0510(60)	0.142
SPFRC1000(60)	0.126	SPFRC1010(60)	0.147
SPFRC1500(30)	0.142	SPFRC1510(30)	0.133
SPFRC1500(60)	0.133	SPFRC1510(60)	0.154
SPFRC1500(80)	0.151	SPFRC1510(80)	0.155
SPFRC0005(60)	0.123	SPFRC0015(60)	0.145
SPFRC0505(60)	0.136	SPFRC0515(60)	0.162
SPFRC1005(60)	0.132	SPFRC1015(60)	0.170
SPFRC1505(60)	0.143	SPFRC1515(60)	0.194

3.4.3. Relationship between carbonated compressive strength and equivalent initial porosity of SPFRC

In this section, the experimental supercritical carbonation depth of SPFRC in Table 5 was compared with the numerical results to calibrate the equivalent initial porosity of the 20 groups of SPFRC specimens. Then the relationship between carbonated compressive strength and the equivalent initial porosity of SPFRC was obtained.

The compressive strength of concrete was affected by the change of pore structure after the carbonation treatment. The molar volume of calcium carbonate is larger than that of calcium hydroxide after carbonation, and the solubility is smaller than that of calcium hydroxide in water. The porosity was reduced, the density and compressive strength of concrete increased after the deposition of calcium carbonate in pores. Then the relationship between the equivalent porosity without the carbonation of SPFRC and the compressive strength of full carbonation were studied in this section. A mathematical model for the relationship between the equivalent initial porosity and the compressive strength of SPFRC was established. The steps of proposing the mathematical model can be summarized as follows. Firstly, the compressive strength of fully carbonated concrete cubes was estimated according to Eq. (2). The one-dimensional mathematical model for the physical-chemical coupling process of supercritical carbonation of cement-based materials was established. Then the equivalent initial porosity was calculated by linear interpolation according to the comparison of carbonation depth of experiment and numerical simulation. Finally, the mathematical model for the relationship between the compressive strength of SPFRC and equivalent initial porosity was proposed as shown in Eq. (11).

The relationship between the compressive strength of concrete and porosity of concrete was proposed by the regression analysis [62] based on the mathematical model [63] as shown in the following equation:

$$f_C = f_{C0} \times (1 - kn_0) \tag{11}$$

where f_C is the fitted value of compressive strength when the initial porosity is n_0, f_{C0} is the value of compressive strength when the initial porosity is 0, k is a coefficient to be determined, n_0 is the equivalent initial porosity.

The relationship between the compressive strength of concrete without carbonation and porosity of concrete was obtained by the regression analysis of the estimated value of equivalent initial porosity in Table 8 and the comprehensive compressive strength of specimens without carbonation, f_{CO}, in Table 6, as shown in Eq. (12).

$$f_C = 82.5 \times (1 - 4.07n_0) \tag{12}$$

in which, f_C is the fitted value of compressive strength when the initial porosity is n_0 without carbonation.

The regression analysis of the compressive strength of SPFRC after the full carbonation and equivalent initial porosity was performed by the estimated value of equivalent initial porosity in Table 8 and the compressive strength of fully carbonated concrete, f_{CC}', in Table 6, as shown in Eq. (13).

$$f_C' = 119.4 \times (1 - 4.07n_0) \tag{13}$$

in which, f_C' is the fitted value of the compressive strength of SPFRC after full carbonation when the initial porosity is n_0.

The comparison of the calculated results by Eq. (12), Eq. (13), and the test results are shown in Fig. 14. As shown in Fig. 14, Eq. (12) and Eq. (13) can be used to describe the relationship between the compressive strength without and after the full carbonation and initial equivalent porosity of SPFRC, respectively. There's a linear relationship between the equivalent initial porosity and compressive strength without carbonation and after full carbonation.

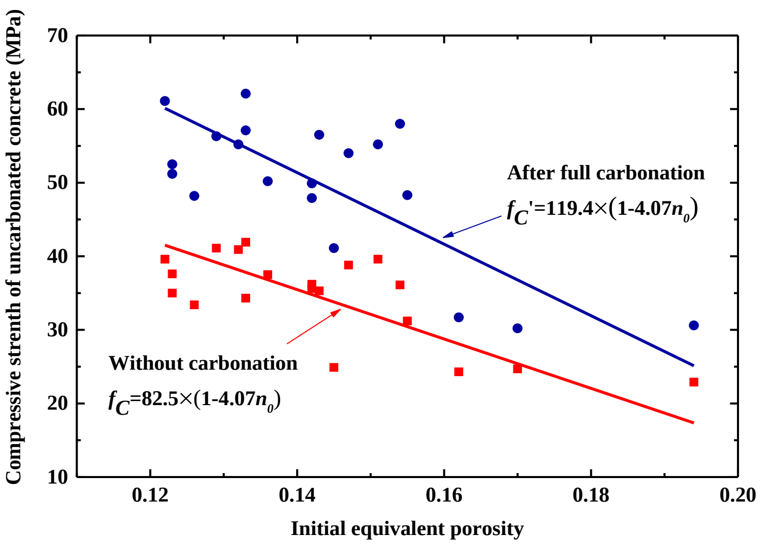

Fig. 14. Regression curves of equivalent initial porosity and compressive strength.

4. Conclusions

In this paper, the supercritical carbonation of steel-polypropylene hybrid fiber reinforced concrete was studied. The main conclusions are as follows:

(1) The compressive strength after carbonation is significantly increased by at least 20%. The maximum relative compressive strength was obtained when the volume fraction of steel fiber and polypropylene fiber was 1.5% and 0.0% and the length-diameter ratio of steel fiber was 60, respectively.

(2) An evaluation formula was proposed to estimate the compressive strength of fully carbonated concrete.

(3) The equivalent initial porosity of SPFRC can be evaluated by the mathematical model of compressive strength after fully carbonated and the equivalent initial porosity of SPFRC.

(4) Further experiments will be carried out to investigate the effects of supercritical carbonation on the porosity of SPFRC and the ITZ between the fibers and matrix. The post cracking behavior of the composite and the mechanical properties are to be evaluated.

Data Availability Statement

Some or all data, models, or code that support the research findings of this study are available from the corresponding author by reasonable request, including the experimental and numerical data.

Acknowledgements

The authors are grateful for the financial support from the Natural Science Foundation of Hubei Province of China (Grant No. 2020CFB272), the Scientific Research Program of Hubei Provincial Department of Education (Grant No. Q20201207), the Opening Foundation of Hubei Key Laboratory of Disaster Prevention and Mitigation (Grant No. 2020KJZ01), the Natural Science Foundation of Yichang (Grant No. A20-3-012) and National Natural Science Foundation of China (Grant No. 51878518).

References

[1] Lee Y, Kang S, Kim J. Pullout Behavior of Inclined Steel Fiber in an Ultra-High Strength Cementitious Matrix. Construction and Building Materials, 2010, 24(10): 2030-2041.

[2] Serafini R, Dantas S R A, Salvador R P, et al. Influence of Fire on Temperature Gradient and Physical-Mechanical Properties of Macro-Synthetic Fiber Reinforced Concrete for Tunnel Linings. Construction and Building Materials, 2019, 214: 254-268.

[3] Xu J, Wu C, Xiang H, et al. Behaviour of Ultra High Performance Fibre Reinforced Concrete Columns Subjected to Blast Loading. Engineering Structures, 2016, 118: 97-107.

[4] Bagherzadeh R, Sadeghi A, Latifi M. Utilizing Polypropylene Fibers to Improve Physical and Mechanical Properties of Concrete. Textile Research Journal, 2011, 82(1): 88-96.

[5] Söylev T A, özturan T. Durability, Physical and Mechanical Properties of Fiber-Reinforced Concretes at Low-Volume Fraction. Construction and Building Materials, 2014, 73: 67-75.

[6] Chakravarthy R, Venkatesan S, Patnaikuni I. Review on Hybrid Fiber Reinforced High Performance High Volume Flyash Concrete. International Journal of Structural and Civil Engineering Research, 2016, 5(1): 39-42.

[7] Bolat H, _imşek O, çullu M, et al. The Effects of Macro Synthetic Fiber Reinforcement Use on Physical and Mechanical Properties of Concrete. Composites Part B: Engineering, 2014, 61: 191-198.

[8] Xu L, Deng F, Chi Y. Nano-Mechanical Behavior of the Interfacial Transition Zone between Steel-Polypropylene Fiber and Cement Paste. Construction and Building Materials, 2017, 145: 619-638.

[9] Ramezanianpour A A, Esmaeili M, Ghahari S A, et al. Laboratory Study on the Effect of Polypropylene Fiber on Durability, and Physical and Mechanical Characteristic of Concrete for Application in Sleepers. Construction and Building Materials, 2013, 44: 411-418.

[10] Frazão C, Camões A, Barros J, et al. Durability of Steel Fiber Reinforced Self-Compacting Concrete. Construction and Building Materials, 2015, 80: 155-166.

[11] Jones M R, Mccarthy A. Preliminary Views on the Potential of Foamed Concrete as a Structural Material. Magazine of Concrete Research, 2005, 57(1): 21-31.

[12] Lihua X, Ping C, Le H, et al. Experimental Research on Bond Properties between Hybrid Steel-Polypropylene Fiber Reinforced Concrete and Deformed Bar. China Civil Engineering Journal, 2015(4):15-22. (in Chinese)

[13] Sufian Badar M, Kupwade-Patil K, Bernal S A, et al. Corrosion of Steel Bars Induced by Accelerated Carbonation in Low and High Calcium Fly Ash Geopolymer Concretes. Construction & building materials, 2014, 61: 79-89.

[14] Bautista A, Paredes E C, Alvarez S M, et al. Welded, Sandblasted, Stainless Steel Corrugated Bars in Non-Carbonated and Carbonated Mortars: A 9-Year Corrosion Study. Corrosion Science, 2016, 102: 363-372.

[15] Stefanoni M, Angst U, Elsener B. Corrosion Rate of Carbon Steel in Carbonated Concrete-a Critical Review. Cement and Concrete Research, 2018, 103: 35-48.

[16] Fernandezbertos M, Simons S, Hills C, et al. A Review of Accelerated Carbonation Technology in the Treatment of Cement-Based Materials and Sequestration of CO_2. Journal of Hazardous Materials, 2004, 112(3): 193-205.

[17] Jerga J. Physico-Mechanical Properties of Carbonated Concrete. Construction and Building Materials, 2004, 18(9): 645-652.

[18] Soroushian P, Won J, Hassan M. Durability Characteristics of CO_2-Cured Cellulose Fiber Reinforced Cement Composites. Construction and Building Materials, 2012, 34: 44-53.

[19] Wu H, Zhang D, Ellis B R, et al. Development of Reactive MgO-Based Engineered Cementitious Composite (ECC) through Accelerated Carbonation Curing. Construction and Building Materials, 2018, 191: 23-31.

[20] Khunthongkeaw J, Tangtermsirikul S, Leelawat T. A Study on Carbonation Depth Prediction for Fly Ash Concrete. Construction and Building Materials, 2006, 20(9): 744-753.

[21] Shen J, Dangla P, Thiery M. Reactive Transport Modeling of CO_2 through Cementitious Materials under CO_2 Geological Storage Conditions. International Journal of Greenhouse Gas Control, 2013, 18: 75-87.

[22] Xuan D, Zhan B, Poon C S. Assessment of Mechanical Properties of Concrete Incorporating Carbonated Recycled Concrete Aggregates. Cement and Concrete Composites, 2016, 65: 67-74.

[23] Thiery M, Dangla P, Belin P, et al. Carbonation Kinetics of a Bed of Recycled Concrete Aggregates: A Laboratory Study on Model Materials. Cement and Concrete Research, 2013, 46: 50-65.

[24] Zhan B, Poon C, Shi C. CO_2 Curing for Improving the Properties of Concrete Blocks Containing Recycled Aggregates. Cement and Concrete Composites, 2013, 42: 1-8.

[25] Zhang J, Shi C, Li Y, et al. Influence of Carbonated Recycled Concrete Aggregate on Properties of Cement Mortar. Construction and Building Materials, 2015, 98: 1-7.

[26] García-González C A, Hidalgo A, Andrade C, et al. Modification of Composition and Microstructure of Portland Cement Pastes as a Result of Natural and Supercritical Carbonation Procedures[J]. Industrial & Engineering Chemistry Research, 2006,45(14):4985-4992.

[27] García-González C A, Hidalgo A, Andrade C, et al. Modification of Composition and Microstructure of Portland Cement Pastes as a Result of Natural and Supercritical Carbonation Procedures. Industrial & Engineering Chemistry Research, 2006, 45(14): 4985-4992.

[28] Kou S, Zhan B, Poon C. Use of a CO_2 Curing Step to Improve the Properties of Concrete Prepared with Recycled Aggregates. Cement and Concrete Composites, 2014, 45: 22-28.

[29] Hay R, Celik K. Accelerated Carbonation of Reactive Magnesium Oxide Cement (RMC)-Based Composite with Supercritical Carbon Dioxide ($SCCO_2$). Journal of Cleaner Production, 2019, 248: 119282.

[30] Short N R, Purnell P, Page C L. Preliminary Investigations into the Supercritical Carbonation of Cement Pastes. Journal of Materials Science, 2001, 36(1): 35-41.

[31] García-González C A, El Grouh N, Hidalgo A, et al. New Insights on the Use of Supercritical Carbon Dioxide for the Accelerated Carbonation of Cement Pastes. The Journal of supercritical fluids, 2008, 43(3): 500-509.

[32] Zha X, Wang H, Xie P, et al. Leaching Resistance of Hazardous Waste Cement Solidification after Accelerated Carbonation. Cement and Concrete Composites, 2016, 72: 125-132.

[33] Venhuis M A, Reardon E J. Vacuum Method for Carbonation of Cementitious Wasteforms. Environmental Science & Technology, 2001, 35(20): 4120-4125.

[34] Zha X, Ning J, Saafi M, et al. Effect of Supercritical Carbonation on the Strength and Heavy Metal Retention of Cement-Solidified Fly Ash. Cement and Concrete Research, 2019, 120: 36-45.

[35] Rubin J B, Carey J W, Taylor C. Enhancement of Cemented Waste Forms by Supercritical CO_2 Carbonation of Standard Portland Cements, 1997: 473-478.

[36] Bao H, Yu M, Liu Y, et al. Experimental and Statistical Study on the Irregularity of Carbonation Depth of Cement Mortar under Supercritical Condition. Construction and Building Materials, 2018, 174: 47-59.

[37] Fernández-Carrasco L, Rius J, Miravitlles C. Supercritical Carbonation of Calcium Aluminate Cement. Cement and Concrete Research, 2008, 38(8): 1033-1037.

[38] Santos S F, Schmidt R, Almeida A E F S, et al. Supercritical Carbonation Treatment on Extruded Fibre-Cement Reinforced with Vegetable Fibres. Cement and Concrete Composites, 2015, 56: 84-94.

[39] Purnell P, Short N R, Page C L. Super-Critical Carbonation of Glass-Fibre Reinforced Cement. Part 1: Mechanical Testing and Chemical Analysis. Composites. Part A, Applied science and manufacturing, 2001, 32(12): 1777-1787.

[40] Smarzewski P. Influence of Basalt-Polypropylene Fibres on Fracture Properties of High Performance Concrete. Composite Structures, 2019, 209: 23-33.

[41] Zha X, Yu M, Ye J, et al. Numerical Modeling of Supercritical Carbonation Process in Cement-Based Materials. Cement and Concrete Research, 2015, 72: 10-20.

[42] Bao H, Yu M, Xu L, et al. Experimental Study and Multi-Physics Modelling of Concrete under Supercritical Carbonation. Construction and Building Materials, 2019, 227: 116680.

[43] Andrade C. Evaluation of the Degree of Carbonation of Concretes in Three Environments. Construction and Building Materials, 2020, 230: 116804.

[44] Beasley K J. Carbon Dating Concrete Cracks. Journal of Performance of Constructed Facilities, 2015, 29(025140021).

[45] Yu M, Bao H, Ye J, et al. The Effect of Random Porosity Field on Supercritical Carbonation of Cement-Based Materials. Construction and Building Materials, 2017, 146: 144-155.

[46] Kim J, Kim C, Yi S, et al. Effect of Carbonation on the Rebound Number and Compressive Strength of Concrete. Cement and Concrete Composites, 2009, 31(2): 139-144.

[47] Jin W, Zhao Y. Durability of Concrete Structures (Second Edition). Science Press, 2014. (in Chinese)

[48] Bao H, Xu G, Wang Q, et al. Investigation on the Distribution Characteristics of Partial Carbonation Zone of Concrete. Journal of Materials in Civil Engineering, 2021, 33(1): 0003548.

[49] Standard, China, JGJ 55-2011. Specification for Mix Proportion Design of Ordinary Concrete. Beijing: China Architecture & Building Press, 2011. (in Chinese)

[50] CECS 38: 2004. Technical Specification for Fiber Reinforced Concrete Structures. Beijing: China Planning Press, 2004. (in Chinese)
[51] CECS 13: 2009. Standard Test Methods for Fiber Reinforced Concrete. Beijing: China Planning Press, 2009. (in Chinese)
[52] Chen Q, Zhu H, Yan Z, et al. A Multiphase Micromechanical Model for Hybrid Fiber Reinforced Concrete Considering the Aggregate and Itz Effects. Construction & building materials, 2016, 114: 839-850.
[53] Xu L, Huang L, Chi Y, et al. Tensile Behavior of Steel-Polypropylene Hybrid Fiber-Reinforced Concrete. ACI Materials Journal, 2016, 113(2): 219-229.
[54] Atiş C D, Karahan O. Properties of Steel Fiber Reinforced Fly Ash Concrete. Construction and Building Materials, 2009, 23(1): 392-399.
[55] Yu K, Yu J, Dai J, et al. Development of Ultra-High Performance Engineered Cementitious Composites Using Polyethylene (PE) Fibers. Construction and Building Materials, 2018, 158: 217-227.
[56] Chen Y, Wang S, Liu B, et al. Effects of Geometrical and Mechanical Properties of Fiber and Matrix on Composite Fracture Toughness. Composite Structures, 2015, 122: 496-506.
[57] Sahoo D R, Maran K, Kumar A. Effect of Steel and Synthetic Fibers on Shear Strength of RC Beams without Shear Stirrups. Construction & building materials, 2015, 83: 150-158.
[58] Li Q. Discussion on Improvement of the Carbonation Performance of Concrete Block with the Cementing Materials of Cement and Fly Ash. Wall Materials Innovation & Energy Saving in Buildings, 2012(10):18-25. (in Chinese)
[59] Baroghel-Bouny V, Thiéry M, Wang X. Modelling of Isothermal Coupled Moisture-Ion Transport in Cementitious Materials. Cement and Concrete Research, 2011, 41(8): 828-841.
[60] Mainguy M, Baroghel-Bouny V, Coussy O. Role of Air Pressure in Drying of Weakly Permeable Materials. 2001, 127(6): 582-592.
[61] Yaman I O, Hearn N, Aktan H M. Active and Non-Active Porosity in Concrete - Part I: Experimental Evidence. Materials and Structures, 2002, 35(246): 102-109.
[62] Jia J, Hu Y, Wang D, et al. Effects of Porosity on the Compressive Strength of Concrete. Concrete, 2015(10): 56-59. (in Chinese)
[63] Bischoff P H, Perry S H. Compressive Behaviour of Concrete at High Strain Rates. Materials and Structures, 1991, 24: 425-450.